Journal of Chemistry and Technologies, 2024, *32*(3), 570-579

Journal of Chemistry and Technologies

pISSN 2663-2934 (Print), ISSN 2663-2942 (Online).

journal homepage: http://chemistry.dnu.dp.ua
editorial e-mail: chem.dnu@gmail.com

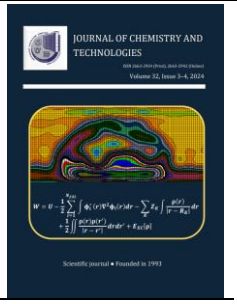

UDC 541.123.3

PHASE EQUILIBRIA IN THE La_2O_3-Lu_2O_3-Ho_2O_3 SYSTEM AT 1500 °C

Olga V. Chudinovych [1, 2*], Oleksandr V. Shyrokov[1], Anatoliy V. Samelyuk[1], Maryna V. Zamula[1], Tetiana A. Kamens'ka[2]

[1] *I. M. Frantsevich Institute for Problems in Materials Science, NAS of Ukraine, 3, Omeliana Pritsaka St., 03142, Kyiv, Ukraine*
[2]*National Technical University of Ukraine «Igor Sikorsky Kyiv Polytechnic Institute», 37, Peremohy Ave., 03056, Kyiv, Ukraine*
Received 11 May 2024; accepted 10 September 2024; available online 20 October 2024

Abstract

The phase equilibria in the La_2O_3–Lu_2O_3–Ho_2O_3 ternary system at 1500 °C were studied by X-ray diffraction (XRD) and scanning electron microscopy (SEM) in the whole concentration range. La_2O_3, Lu_2O_3, and Ho_2O_3 (99.99 %) were used as starting substances. The experimental samples were prepared with a concentration step of 1–5 mol%. The oxides were dissolved in HNO_3 (1 : 1) followed by evaporation of the solutions and decomposition of nitrates at 800 °C for 2 hours. The samples were heat treated at 1500 °C (for 70 h) in air. The phase composition of the test samples studied by X-ray diffraction (XRD, DRON-3), microstructural phase and electron microprobe X–ray (Superprobe-733, JEOL, Japan, Palo Alto, CA) analyses. Solid solutions based on various polymorphic forms of original oxides and ordered $LaLuO_3$ phase were detected in the system. No new phases were found in the system. The isothermal cross-sections of the La_2O_3–Lu_2O_3–Ho_2O_3 phase diagram at 1500 °C are characterized by the presence of four single-phase (A-La_2O_3, B-La_2O_3, R, C-Lu_2O_3 (Ho_2O_3)), five two-phase (C + R, A + R, B + A, B + R, B + C) and two three-phase (A + R+ B, B + R + C) regions. Solubility limits are determined and concentration dependences of periods also lattice parameters of the unit cell of phases formed in the system are constructed. The range of homogeneity of solid solutions based on the R-phase extends from 0 to 8 mol% Ho_2O_3 and from ~47 to 54 mol% La_2O_3 at 1500 °C. Lu and Ho oxides form an continuous series of C-REE oxide solid solutions.

Keywords: phase equilibria; lanthana; lutetia; holmia; isothermal section; solid solutions; lattice parameters.

ФАЗОВІ РІВНОВАГИ У СИСТЕМІ La_2O_3-Lu_2O_3-Ho_2O_3 ЗА 1500 °C

Ольга В. Чудінович[1,2], Олександр В. Широков[1], Анатолій В. Самелюк[1], Марина В. Замула[1], Тетяна А. Каменська[2]

[1]*Інститут проблем матеріалознавства ім. І.М. Францевича НАН України, вул. Омеляна Пріцака, 3, Київ, Україна, 03142*
[2]*Національний технічний університет України "Київський політехнічний інститут імені Ігоря Сікорського", просп. Перемоги, 37, м. Київ, Україна, 03056*

Анотація

Досліджено фазову взаємодію у потрійній системі La_2O_3–Lu_2O_3–Ho_2O_3 за 1500 °C у всьому інтервалі концентрацій. Оксиди La, Lu, Ho (99.99 %) використовували як вихідні речовини. Концентраційний крок досліджуваних зразків – 1–5 мол. %. Вихідні оксиди розчиняли в нітратній кислоті (1 : 1) з подальшим випаровуванням розчинів і розкладанням нітратів при 800 °C протягом 2 годин. Термообробку зразків проводили при 1500 °C (протягом 70 год) у повітрі. Фазовий склад зразків вивчали за допомогою рентгенівської дифракції (XRD, DRON-3), мікроструктурного фазового аналізу (Superprobe-733, JEOL, Японія, Пало-Альто, Каліфорнія). У потрійній системі La_2O_3–Lu_2O_3–Ho_2O_3 утворюються тверді розчини на основі різних поліморфних модифікацій вихідних оксидів і впорядкованої фази типу перовскіту ($LaLuO_3$). У системі нові фази не утворюються. Ізотермічний переріз системи La_2O_3–Lu_2O_3–Ho_2O_3 за 1500 °C характеризуються наявністю чотирьох однофазних (A-La_2O_3, B-La_2O_3, R, C-Lu_2O_3 (Ho_2O_3)), п'яти двофазних (C + R, A + R, B + A, B + R, B + C) і двох трифазних (A + R+ B, B + R + C) областей. Побудовано концентраційні залежності параметрів елементарної комірки фаз, що утворюються у системі. Область гомогенності твердих розчинів на основі R-фази простягається від 0 до 8 моль % Ho_2O_3 і від ~47 до 54 мол% La_2O_3 при 1500 °C. Оксиди лютецію та гольмію утворюють неперервний ряд твердих розчинів на основі кубічної модифікації оксидів РЗЕ.

Ключові слова: фазові рівноваги; оксиди лантану; лютецію; гольмію; ізотермічний переріз; тверді розчини; параметри елементарної комірки.

**Corresponding author: e-mail: chudinovych_olia@ukr.net*

doi: 10.15421/jchemtech.v32i3.303869

Journal of Chemistry and Technologies, 2024, *32*(3), 570-579

Introduction

Recently, significant attention has been paid to research on developing phosphors based on rare earth elements. These materials have a wide range of applications in such fields as solar cells, optical fiber communication systems, solid-state lasers, display panels, and electron beam tubes (CRT) [1–9]. The oxides of rare earth elements are chemically stable with low phonon energy, which allows RE^{3+} ions to be doped with other ions such as Ho^{3+}, Eu^{3+}, Ce^{3+}, Tb^{3+}, Tm^{3+}, and Sm^{3+}. For example, lanthanum oxide (La_2O_3) has unique characteristics such as a wide band gap of 4.3 eV, high stability, close ionic radius to other RE ions, luminescence, and low phonon energy ~400 cm^{-1} [9]. Doping lanthanum oxide with different REE makes it attractive for photoconverters due to its optical, luminescent, and dielectric properties. Lutetium oxide is used for scintillation materials [10]. Lanthanum oxide is used for special high-tech glasses, transmitting infrared and absorbing ultraviolet rays [11].

The phase equilibria in the La_2O_3–Lu_2O_3 system were examined by X-ray diffraction and thermal analysis at high temperatures [12]. The melt was crystallized at temperatures above 2000 °C to obtain perovskite-like $LaLuO_3$ single crystals. The orthorhombic cell parameters are a = 6.00 nm, b = 5.79 mn, c = 8.35 nm and space group is Pnam [12]. The paper [13] provides calculations of oxygen vacancies in La_2O_3, Lu_2O_3, and $LaLuO_3$ but there was no data on phase equilibria. The La_2O_3–Lu_2O_3 system at 1500 °C (and at 1600°C) is characterized by the hexagonal (A) modification of lanthanum oxide with the solubility of Lu_2O_3 9 mol.% (and 9 mol.% at 1600 °C), cubic (C) modification of lutetium oxide with the solubility of A-La_2O_3 4 mol.% (and 7 mol. % at 1600 °C), and ordered perovskite-type $LaLuO_3$ (R) phase in the range 48–56 mol.% Lu_2O_3 (and 48–55 mol.% Lu_2O_3 at 1600 °C) [14].

Phase relations and phase structures formed in the La_2O_3–Ho_2O_3 binary system were studied in [16–19]. It should be noted that research in this system was conducted both experimentally [17–19], and using thermodynamic calculations [16]. In [17], the existence of several types of solid solutions was established: high-temperature cubic (*X*), hexagonal (*A* and *H*), monoclinic (*B*), and low-temperature cubic *C*–type Ln_2O_3. In [19] it was found that below the temperature of 1300 °C the formation of an ordered phase with a structure of the perovskite $LaHoO_3$ is observed. The lattice parameters of the ordered phase with the structure of the perovskite–type a = 0.5885 nm, b = 0.6094 nm, c = 0.8508 nm are established. At the same time, according to the results of thermodynamic calculations, the existence of an ordered phase with a perovskite–type structure has not been established [16]. The liquidity curve of the La_2O_3–Ho_2O_3 binary system is characterized by the formation of a minimum near the composition of 20 mol% La_2O_3 [17–18]. It is established that in the La_2O_3–Ho_2O_3 system at 1500 °C three types of solid solutions are formed: based on hexagonal modification A–La_2O_3, monoclinic modification B–Ho_2O_3 and cubic modification C–Ho_2O_3 which are separated by two–phase fields (A + B) and (B + C), respectively [15]. The boundaries of the regions of homogeneity of solid solutions based on A–La_2O_3 are determined by compositions containing 25–30 mol% Ho_2O_3 at 1500 °C [15]. It is established that the region of homogeneity of cubic solid solutions of C–type extends from 100 to 82 mol% Ho_2O_3 at 1500 °C [15].

The phase diagrams of the system consisted of oxides at the end of the lanthanide series feature infinite solid solutions based on A, B, C, H, and X modifications of REE oxides [20–22].

Phase equilibria in binary systems based on oxides of rare earth elements have been studied completely [23–27]. Information on phase equilibria in the ternary La_2O_3–Lu_2O_3–Ho_2O_3 system is absent and requires further research. The purpose of this work is to study the interaction of lanthanum, lutetium and holmium oxides at 1500 °C in the whole concentration range and to construct the corresponding isothermal cross–section of the phase diagram.

Experimental

Lanthanum oxide, La_2O_3, lutetium oxide, Lu_2O_3, holmium oxide, Ho_2O_3 (all 99.99 %), and analytical-grade nitric acid were used as the starting materials. In total 100 compositions in the La_2O_3-Lu_2O_3-Ho_2O_3 system were prepared in the present work for experimental analysis. The experimental samples were prepared in step 1-5 mol% from nitrate solutions with their subsequent evaporation and decomposition at 800 °C for 2 h. Powders were pressed at 10 MPa into pellets of 5 mm in diameter and 4 mm in height. To study phase relationships at 1500 °C thermal treatment of as-prepared samples was carried out in two stages: at 1100 °C (for 980 h in air) and then at 1500 °C (for 70 h in air) in the furnaces with heating elements based on Fecral (H23U5T) and Superkanthal ($MoSi_2$), respectively. The heating rate was 3 °C/min^{-1}.

Journal of Chemistry and Technologies, 2024, *32*(3), 570-579

X-ray diffraction analysis of the samples was performed by a powder method at room temperature (CuKα radiation). The scanning speed of 0.05–0.1° 2θ/min was employed in the 15° to 80° 2θ range. The effective precision of the measurements was ± 0.0002 nm. Lattice parameters were refined by least squares fitting using the LATTIC program. The uncertainty in the lattice parameter of cubic phases was within 0.0002 nm. Phase composition has been determined with the aid of International powder standards (JSPDS International Center for Diffraction Data 1999).

Microstructures were examined on polished sections of annealed samples by electron-probe x-ray microanalysis (EPXMA) in backscattered electron (COMPO) and secondary electron (SEI) modes.

Results and discussion

The tested samples were made into five beams: Lu_2O_3–(50 mol % La_2O_3–50 mol % Ho_2O_3), La_2O_3–(50 mol% Lu_2O_3–50 mol% Ho_2O_3), Ho_2O_3–(50 mol% Lu_2O_3–50 mo l% La_2O_3), Lu_2O_3–(40 mol% La_2O_3–60 mol% Ho_2O_3), Lu_2O_3–(70 mol% La_2O_3–30 mol% Ho_2O_3). Chemical and phase compositions of the samples annealed at 1500°C and the lattice parameters of the phases that are in equilibrium at this temperature are summarized in Table. The results were used to construct the isothermal section of the La_2O_3–Lu_2O_3–Ho_2O_3 phase diagram at 1500 °C (Fig. 1).

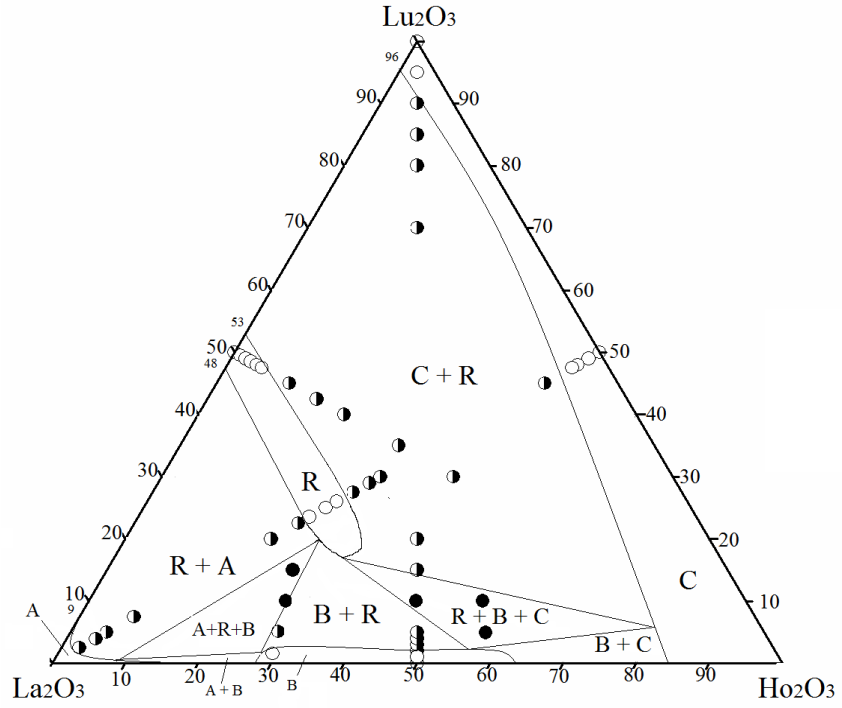

Fig. 1. The isothermal section at 1500 °C for the system La_2O_3–Lu_2O_3–Ho_2O_3 (○ – single-phase, ◐ – two-phase and ● – three-phase regions)

Table

Phase composition and lattice parameters of the phases in the La_2O_3–Lu_2O_3–Ho_2O_3 samples, annealed at 1500° C

Chemical composition, mol %			Phases by XRD, lattice parameters of the phases, nm	Lattice parameters of the phases σ ± 0.0002, nm			
				R			<C>
Lu_2O_3	La_2O_3	Ho_2O_3		*a*	*b*	*c*	*a*
1	2	3	4	5	6	7	8
Section Lu_2O_3—(50 mol % La_2O_3—50 mol % Ho_2O_3)							
0	50	50	<B> (*a* =1.465, *b* = 0.362, *c* = 0.872)				
1	49.5	49.5	<B> (*a* =1.468, *b* = 0.363, *c* = 0.873)				
2	49	49	<B> (*a* =1.485, *b* = 0.366, *c* = 0.871)+ R	0.586	0.608	0.844	
3	48.5	48.5	<B> (*a* =1.467, *b* = 0.361, *c* = 0.878)+ R	0.600	0.594	0.845	
5	47.5	47.5	<B> (*a* =1.451, *b* = 0.362, *c* = 0.876)+ R	0.585	0.608	0.845	

Continuation of Table

10	45	45	<B> (*a* =1.631, *b* = 0.359, *c* = 0.911)+ R + <C>	0,588	0,604	0,843	1,054
20	40	40	R + <C>				1.052
70	15	15	R + <C>	0.582	0.602	0.843	1.043
80	10	10	R + <C>	0.579	0.601	0.854	1.041
85	7.5	7.5	R + <C>	0.579	0.596	0.854	1.041
90	5	5	Rtr + <C>				1.040
95	2.5	2.5	<C>				1.039
100	0	0	<C>				1.039
Section Ho_2O_3—(50 mol % La_2O_3—50 mol % Lu_2O_3)							
49.5	49.5	1	R	0.580	0.599	0.839	
49	49	2	R	0.583	0.599	0.835	
48.5	48.5	3	R	0.581	0.599	0.836	
48	48	4	R	0.582	0.599	0.837	
47.5	47.5	5	R	0.581	0.599	0.822	
45	45	10	R + <C>tr	0.581	0.600	0.837	
42.5	42.5	15	R + <C>	0.539	0.604	0.873	
40	40	20	R + <C>	0.581	0.600	0.839	1.049
30	30	40	R + <C>	0.585	0.607	0.843	1.061
Section Lu_2O_3—(70 mol % La_2O_3—30 mol % Ho_2O_3)							
3	67,9	29,1	<B> (*a* =1.488, *b* = 0.370, *c* = 0.835)				
5	66,5	28,5	<B> (*a* =1.511, *b* = 0.370, *c* = 0.837) + R				
10	63	27	<B> (*a* =1.408, *b* = 0.369, *c* = 0.912) + R +<A> (*a* = 0.652, *b* = 0.379)				
15	59,5	25,5	<B> (*a* =1.477, *b* = 0.352, *c* = 0.916) + R + <A> (*a* = 0.654, *b* = 0.378)				
Section La_2O_3—(50 mol % Lu_2O_3 — 50 mol % Ho_2O_3)							
50	0	50	<C>				1.047
49	2	49	<C>	—	—	—	1.049
47.5	5	47.5	R tr + <C>				1.051
45	10	45	R tr + <C>				1.051
30	40	30	R + <C>	0.603	0.602	0.772	1.054
29	42	29	R + <C>	0.591	0.605	0.783	1.052
27.5	45	27.5	R + <C>	0.584	0.605	0.838	1.049
26	48	26	R	0.585	0.6045	0.841	
23.5	53	23.5	R	0.584	0.6035	0.840	
22.5	55	22.5	R + <A> (a=0.655, c=0.372)	0.584	0.603	0.841	
20	60	20	R + <A> (a=0.649, c=0.379)	0.583	0.603	0.841	
7,5	85	7.5	R + <A> (a=0.649, c=0.381)	0.580	0.603	0.843	
5	90	5	R + <A> (a=0.646, c=0.382)	0.583	0.601	0.838	
4	92	4	Rtr + <A> (a=0.648, c=0.383)				
2.5	95	2.5	Rtr + <A> (a=0.650, c=0.382)				
Section Lu_2O_3—(40 mol % La_2O_3—60 mol % Ho_2O_3)							
5	38	57	<B> (*a* =1.753, *b* = 0.365, *c* = 0.869) + <C>				1.068
10	36	54	<B> (*a* =1.703, *b* = 0.363, *c* = 0.862) + <C> + R	0.586	0.604	0.849	
6	65	29	<B> (*a* =1.484, *b* = 0.363, *c* = 0.889) + R	0.608	0.587	0.863	

An examination of the X–ray data and microstructural analysis has not identified any new phase in the La_2O_3–Lu_2O_3–Ho_2O_3 system. The phase equilibria in the ternary La_2O_3–Lu_2O_3–Ho_2O_3 system at 1500 °C are determined by the boundary of binaries and four homogeneity fields of solid solutions have been identified. It has been found that in the system La_2O_3–Lu_2O_3–Ho_2O_3 the following solid solutions are in equilibria at 1500 °C based on the cubic (C) Lu_2O_3(Ho_2O_3), hexagonal (A) and monoclinic (B) La_2O_3, as well as ordered phase of perovskite–type of $LaLuO_3$ (R).

Lu and Ho oxides form series of C–REE oxide solid solutions. This field ranges along the Lu_2O_3–Ho_2O_3 side of the composition triangle. The C–phase homogeneity range extends in compliance with its solubility limits in the binary La_2O_3–Lu_2O_3, La_2O_3–Ho_2O_3, and Lu_2O_3–Ho_2O_3 systems. This direction of the homogeneity range of the C-

Journal of Chemistry and Technologies, 2024, *32*(3), 570-579

phase indicates that Lu^{3+} ions are predominantly replaced by Ho^{3+} ions and vice versa, without charge compensation. Using the concentration dependences of the unit cell parameters, it was established that the range of homogeneity of solid solutions based on the C–phase extends from 94 to 100 mol% Lu_2O_3 at 1500 °C in the section Lu_2O_3–(50 mol% La_2O_3–50 mol% Ho_2O_3) and from 0 to 4 mol% La_2O_3 at 1500 °C in the section La_2O_3–(50 mol% Lu_2O_3–50 mol% Ho_2O_3) (Fig. 2, 3).

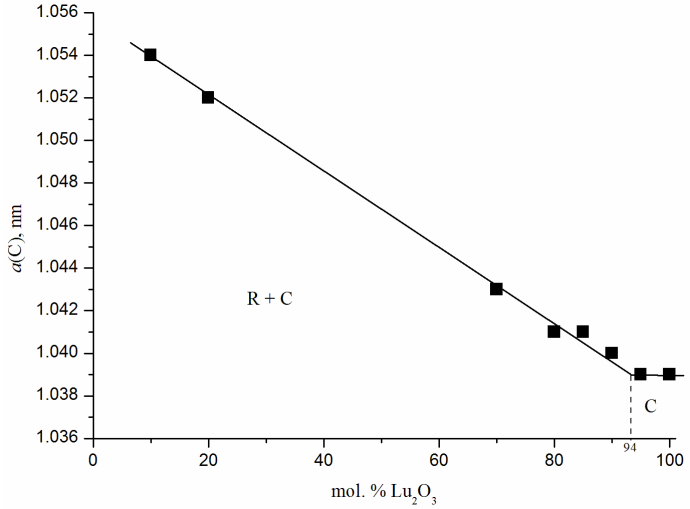

Fig. 2. Concentration dependence of lattice parameters for solid solutions based on C–type of rare–earth oxides along the section of Lu_2O_3– (50 mol % Ho_2O_3–50 mol % La_2O_3) in the system La_2O_3–Lu_2O_3–Ho_2O_3 heat-treated at 1500 °C

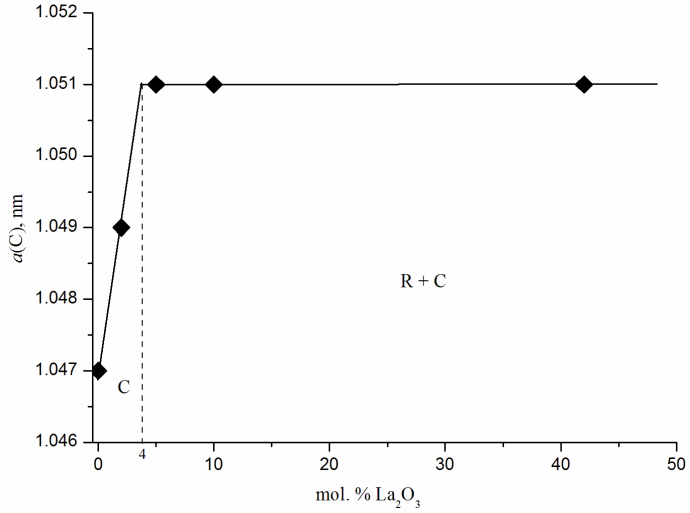

Fig. 3. Concentration dependence of lattice parameters for solid solutions based on C–type of rare–earth oxides along the section of La_2O_3–(50 mol % Ho_2O_3–50 mol % Lu_2O_3) in the system La_2O_3–Lu_2O_3–Ho_2O_3 heat–treated at 1500 °C

The lattice parameters of the unit cell C–phase vary from a= 1.039 nm in sample, containing 95 mol% Lu_2O_3–2.5 mol% La_2O_3–2.5 mol% Ho_2O_3 to a= 1.041 nm in two-phase sample (C + R), containing 85 mol% Lu_2O_3–7.5 mol% La_2O_3–7.5 mol% Ho_2O_3 in the section Lu_2O_3–(50 mol% La_2O_3–50 mol% Ho_2O_3). The lattice parameters of the unit cell C-phase vary from a= 1.049 nm in sample, containing 49 mol% Lu_2O_3–2 mol% La_2O_3–49 mol% Ho_2O_3 to a= 1.054 nm in two-phase sample (C + R), containing 30 mol% Lu_2O_3–40 mol% La_2O_3–30 mol% Ho_2O_3 in the section La_2O_3–(50 mol% Lu_2O_3–50 mol% Ho_2O_3).

The cubic solid solutions formation is characteristic of oxides at the end of the lanthanide series (Yb_2O_3, Er_2O_3, Ho_2O_3, Lu_2O_3). For comparison, in the La_2O_3–Lu_2O_3–Yb_2O_3 system at 1500 [26] and 1600 °C [25] and La_2O_3–Lu_2O_3–Er_2O_3 system at 1500 and 1600 °C [27], a continuous series of solid solutions based on the C-form of REE oxides is also formed.

The X–ray diffraction patterns for the samples in the La_2O_3–Lu_2O_3–Ho_2O_3 system at 1500 °C are presented in Figure 4.

Journal of Chemistry and Technologies, 2024, *32*(3), 570-579

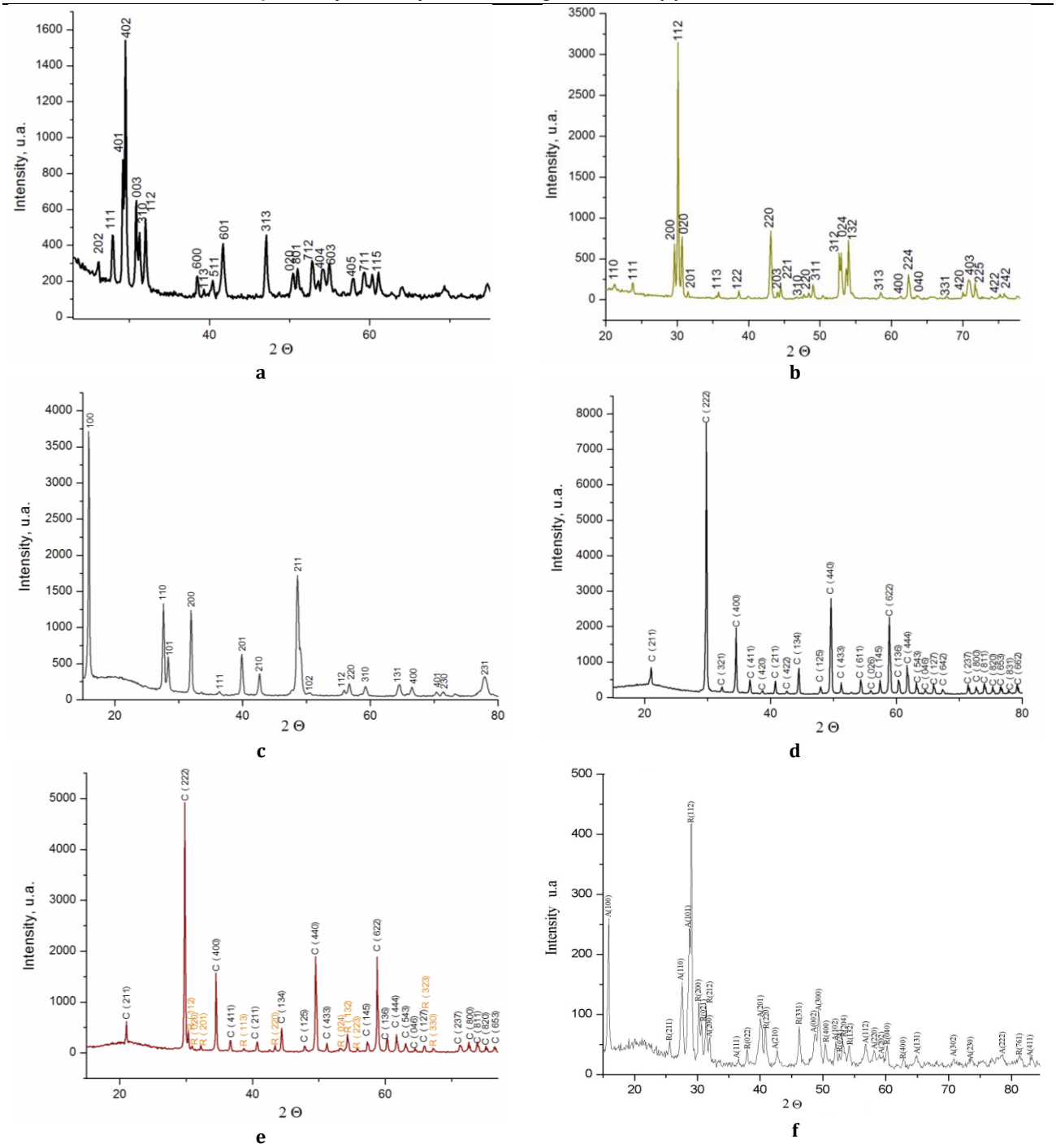

a) 1mol % Lu_2O_3–49.5 mol % La_2O_3–49.5 mol % Ho_2O_3, (B); b) 48 mol % Lu_2O_3–48 mol % La_2O_3–4 mol % Ho_2O_3, (R); c) 4mol % Lu_2O_3–92 mol % La_2O_3–4 mol % Ho_2O_3, (A); d) 95 mol % Lu_2O_3–2.5 mol % La_2O_3–2.5 mol % Ho_2O_3, (C); e) 90 mol % Lu_2O_3–5 mol % La_2O_3–5 mol % Ho_2O_3, (R+C); f) 20 mol % Lu_2O_3–60 mol % La_2O_3–20 mol % Ho_2O_3, (R+C)

Fig. 4 XRD patterns of the samples for the La_2O_3–Lu_2O_3–Ho_2O_3 system heat-treated at 1500 ºC

In the ternary system La_2O_3–Lu_2O_3–Ho_2O_3 at 1500 °C, the ordered phase of perovskite–type with rhombic distortion has been revealed. The boundaries of the homogeneity field of the ordered phase LaLuO3 (R) at 1500 °C have a substantial extension (48–53 mol % Lu_2O_3) along the side of the La_2O_3–Lu_2O_3 concentration triangle. The stability of the R–phase by the addition of a third component (Ho_2O_3) increases markedly in comparison with the binary system La_2O_3–Lu_2O_3. The field of solid solutions of the perovskite-type phase is directed toward the opposite side of the concentration triangle corresponding binary Ho_2O_3–Lu_2O_3 system. The maximum solubility of holmium oxide in the R–phase is ~8 mol% along section Ho_2O_3–(50 mol % La_2O_3–50 mol% Lu_2O_3) (Fig. 5). The lattice parameters of the unit cell R–phase vary from a =

Journal of Chemistry and Technologies, 2024, *32*(3), 570-579

0.580 nm, b = 0. 599 nm, c = 0.839 nm in the single–phase sample, containing 49.5 mol % La_2O_3–49.5 mol % Lu_2O_3–1 mol % Ho_2O_3 to a = 0.585 nm, b = 0.607 nm, c = 0.843 nm in the two–phase sample (R + C), containing 30 mol % La_2O_3–30 mol % Lu_2O_3–40 mol % Ho_2O_3

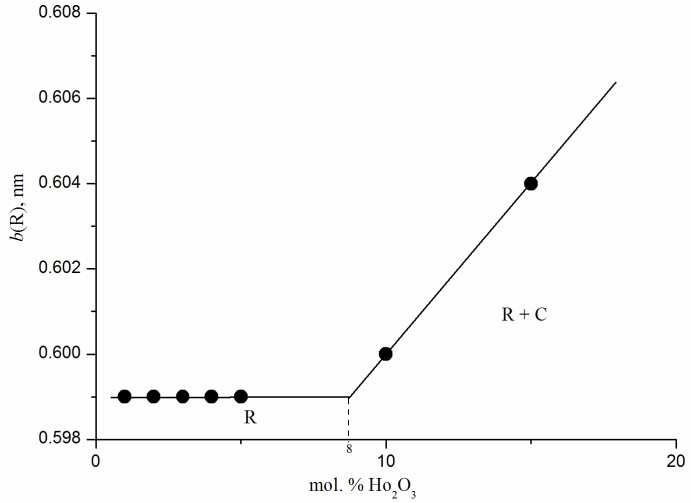

Fig. 5. Concentration dependence of lattice parameters (*b*) for solid solutions based on R–phase along the section of Ho_2O_3– (50 mol % La_2O_3–50 mol % Lu_2O_3) in the system La_2O_3–Lu_2O_3–Ho_2O_3 heat–treated at 1500 °C

Using the fig. 1,3,5,6, it was established that the range of homogeneity of solid solutions based on the R–phase extends from 47 to 54 mol% La_2O_3 at 1500°C in the section La_2O_3–(50 mol% Lu_2O_3–50 mol% Ho_2O_3) (Fig. 6). The perovskite–type phase exists in a two phase (B + R, C + R, A + R) and three–phase (B + A + R, B + C + R) fields.

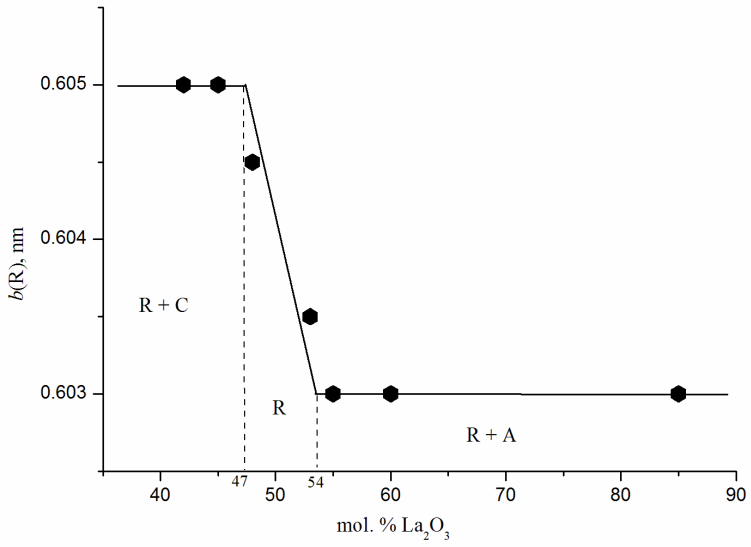

Fig. 6. Concentration dependence of lattice parameters (*b*) for solid solutions based on R–phase along the section of La_2O_3–(50 mol % Ho_2O_3–50 mol % Lu_2O_3) in the system La_2O_3–Lu_2O_3–Ho_2O_3 heat–treated at 1500 °C

The formation of the R–phase was observed in some systems La_2O_3–Lu_2O_3–Yb_2O_3, La_2O_3–Lu_2O_3–Er_2O_3, La_2O_3–Y_2O_3–Nd_2O_3, La_2O_3–Y_2O_3–Sm_2O_3, La_2O_3–Y_2O_3–Er_2O_3 and La_2O_3–Y_2O_3–Yb_2O_3 at 1500 °C [25–27]. Similar to this system, in the La_2O_3–Y_2O_3–Nd_2O_3 system at 1500 °C, a region of solid solutions is formed based on an ordered phase with a perovskite–type structure. The maximum solubility of neodymium oxide in the R–phase is ~7 mol % along section Nd_2O_3–(50 mol% La_2O_3–50 mol % Y_2O_3) [23].

In contrast, in the La_2O_3–Lu_2O_3–Yb_2O_3 [26], La_2O_3–Lu_2O_3–Er_2O_3 [27] and La_2O_3–Y_2O_3–Er_2O_3 systems at 1500 °C, continuous series of solid solutions based on an ordered phase with a perovskite–type structure are also formed. This indicates the mutual substitution of Ln_1^{3+} ions by Ln_2^{3+}, and vice versa.

Due to the thermodynamic stability of the ordered R–phase in the La_2O_3–Lu_2O_3–Ho_2O_3 system the two three–phase field triangle of transformation (B + C + R, R + A+ B) occur.

Journal of Chemistry and Technologies, 2024, *32*(3), 570-579

Depending on the holmium oxide content, the microstructural changes from the single–phase samples (R) to the two–phase samples (C + R) can be followed in Fig. 7. In Fig. 7 shows the microstructures of the samples section on the Ho_2O_3–(50 mol % La_2O_3 – 50 mol % Lu_2O_3) section. The C–phase is light and the R–phase is dark. With increasing holmium oxide content, the amount of the C–type phase increases (Fig. 7).

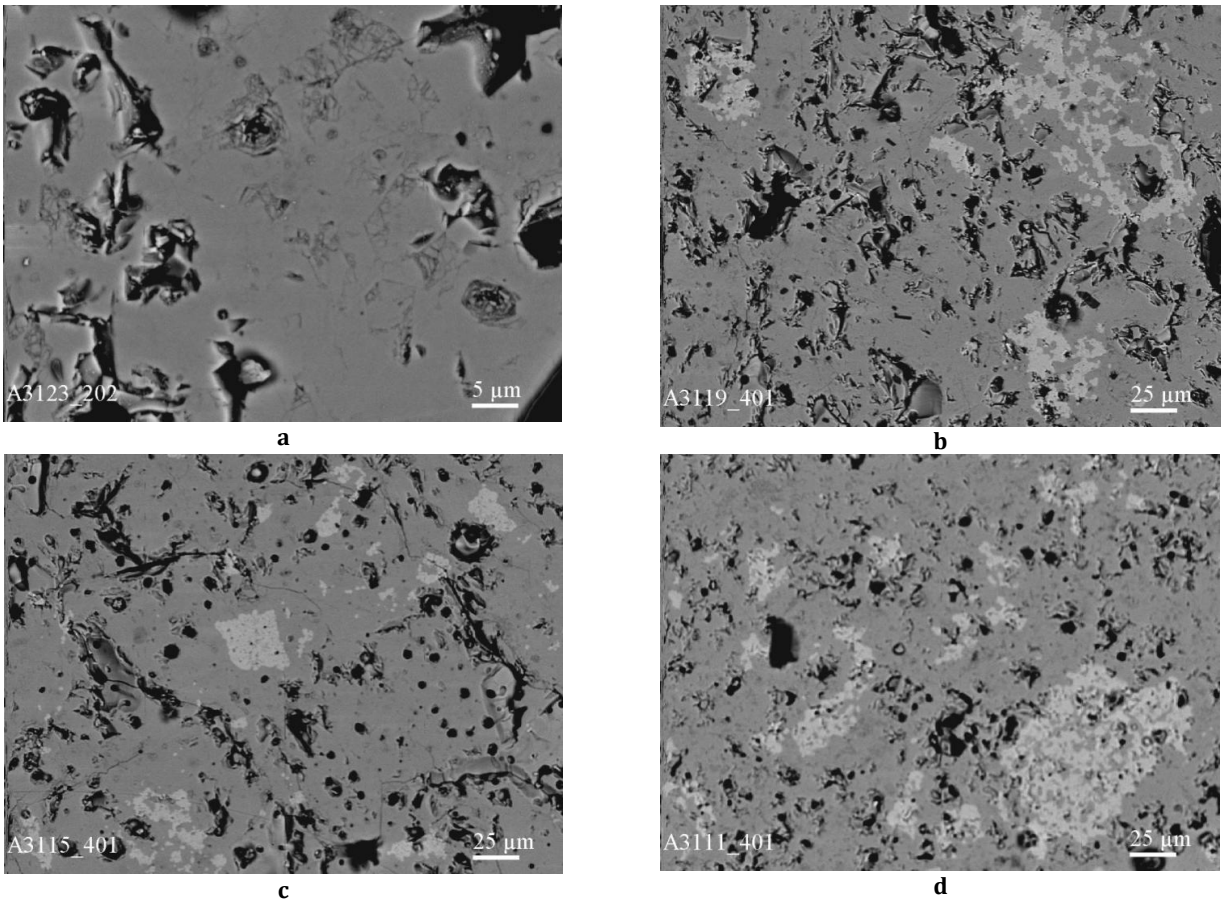

a) 47.5 mol % Lu_2O_3–47.5 mol % La_2O_3 –5 mol % Ho_2O_3 (R); b) 45 mol % Lu_2O_3–45 mol % La_2O_3–10 mol % Ho_2O_3 (R +C); c) 42.5 mol % Lu_2O_3–42.5 mol % La_2O_3–15 mol % Ho_2O_3 (R +C); d) 40 mol % Lu_2O_3–40 mol % La_2O_3–20 mol % Ho_2O_3 (R +C), dark phase – R, light phase – <C>–Lu_2O_3, black – pores

Fig. 7. SEM microstructures of the samples in the definite field of compositions of the system La_2O_3–Lu_2O_3–Ho_2O_3 heat–treated at 1500 °C

In the region with a high content of La_2O_3 solid solutions are formed based on the hexagonal modification of lanthanum oxide. For XRD data in these samples, instead of the hexagonal modification of La_2O_3, the hexagonal modification of A–$La(OH)_3$ is provided (Fig. 4). This arose in this work, however, proper storage and prompt investigation after annealing would have made it possible to obtain A–La_2O_3. Nevertheless, since this applies only to A–La_2O_3 in the investigated system, the results obtained for $La(OH)_3$ can be attributed to A–La_2O_3. The homogeneity range of the A–phase is not extensive and is concave in the direction of decreasing lutetium oxide content and passes under its solubility limits in the boundary binary La_2O_3–Lu_2O_3 and La_2O_3–Ho_2O_3 systems. The solubility of lutetium oxide in the A–phase is ~4 mol % along section La_2O_3–(50 mol. % Lu_2O_3–50 mol. % Ho_2O_3) (Fig. 1). This type of deviation from additivity corresponds to contraction of hexagonal lattice on the appearance of smaller Lu^{3+} ion in the La^{3+} site.

The system forms a homogeneity field of solid solutions based on the monoclinic modification of B–La_2O_3.The homogeneity range of the B–phase passes under its solubility limits in the boundary binary system. The homogeneity range of the B–phase at section Lu_2O_3 – (50 mol. % La_2O_3 – 50 mol% Ho_2O_3) extends from 0 to 1 mol % Lu_2O_3 at 1500 °C (Fig. 1). The X–ray diffraction patterns and microstructures of solid solutions based on the B–phase are presented in Fig. 4 and Fig. 8, respectively.

Journal of Chemistry and Technologies, 2024, *32*(3), 570-579

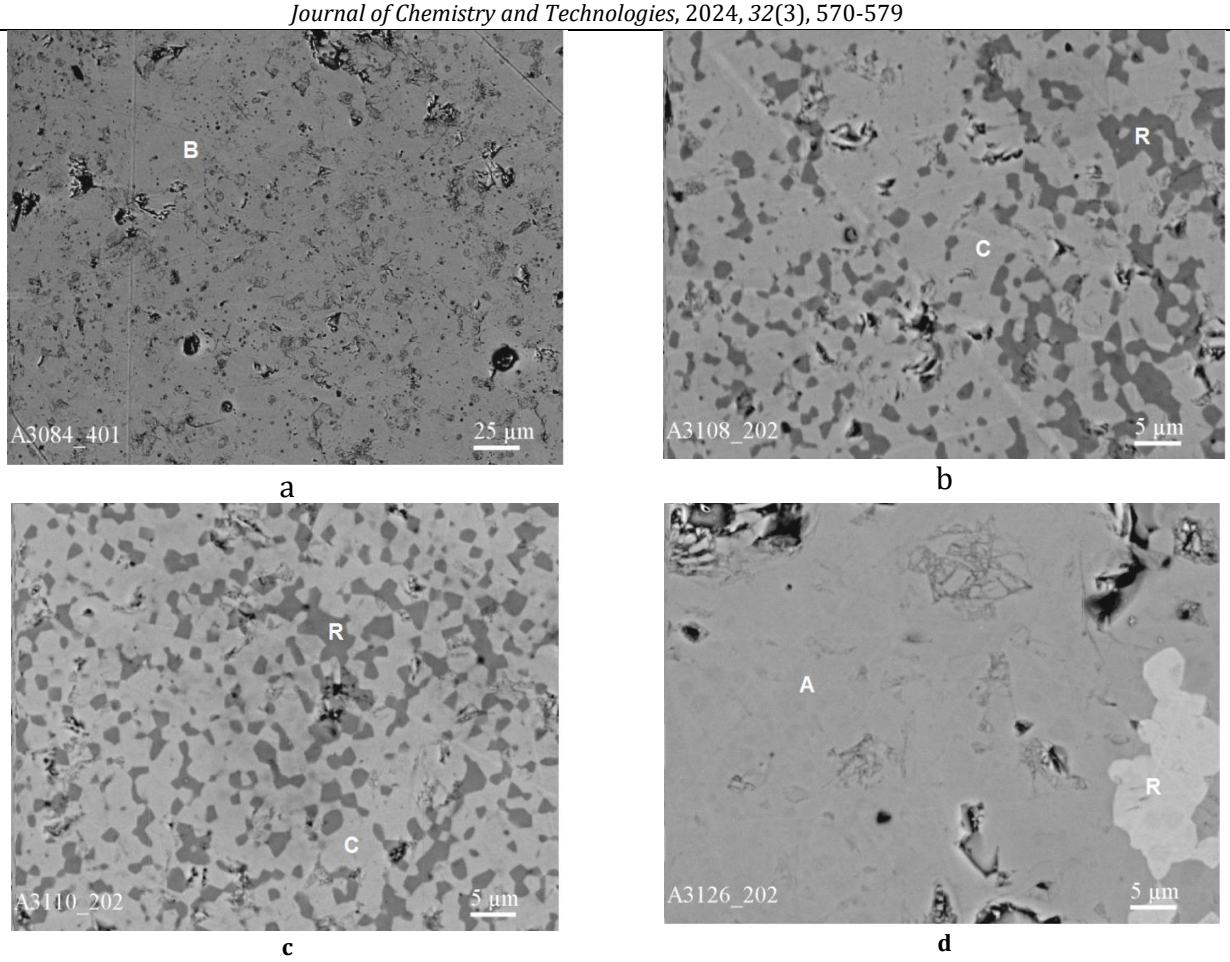

a) 1 mol% Lu_2O_3–49.5 mol% La_2O_3 –49.5 mol% Ho_2O_3; b) 80 mol% Lu_2O_3–10 mol% La_2O_3–10 mol% Ho_2O_3; c) 70 mol% Lu_2O_3–15 mol% La_2O_3–15 mol% Ho_2O_3 (R +C); d) 2.5 mol% Lu_2O_3–95 mol% La_2O_3–2.5 mol% Ho_2O_3 (R +C); R – R–phase, C – <C>–Lu_2O_3, A – <A>–La_2O_3, B – <B>–La_2O_3, black – pores

Fig. 8. SEM microstructures of the samples in the definite field of compositions of the system La_2O_3–Lu_2O_3–Ho_2O_3 heat-treated at 1500 °C

Conclusions

Phase relationships have been studied in the La_2O_3–Lu_2O_3–Ho_2O_3 system at 1500 °C. It has been established that solid state interactions between three oxides resulted in the formation of extended fields of solid solutions based on A–La_2O_3, B–La_2O_3, C–Lu_2O_3(Ho_2O_3)), as well as the ordered phase of perovskite–type $LaLuO_3$ (R). The largest homogeneity field is represented by the continuous solid solutions based on the cubic (C) modification of REO. R–phase is the ordered phase in the ternary system that exists in a wider concentration range than in the boundary binary system. The isothermal section of the La_2O_3–Lu_2O_3–Ho_2O_3 system at 1500 °C is characterized by a two three–phase tie–line triangle (B + C + R, R + B + A), the four one–phase fields (A–La_2O_3, B–La_2O_3, R, C–Lu_2O_3(Ho_2O_3)) corresponding to pure solid solutions based on input components and two–phase fields (A + B, B + R, C + R, B + C, A + R) between them.

References

[1] Milisavljevic, I., Zhang, M., Jiang, Q., Liu, Q., Wu, Y. (2025). Transparent Electro-Optic Ceramics: processing, materials, and applications, *Journal of Materiomics, 11*(2), 100872. https://doi.org/10.1016/j.jmat.2024.04.002

[2] Peng, L., Yang, J., Han, T., Lang, T., Cao, S., Liu, B., Qiang, Q., Chen, W. (2023). Tunable emission and high chromogenic laser lighting of transparent ceramics for high-brightness white LEDs/LDs, *Journal of Luminescence, 263*, 119987, https://doi.org/10.1016/j.jlumin.2023.119987

[3] Mo, J., Zhang, L., Hu, C., Wang, Y., Chen, H., Li, X., Wu, J., Cheng, Z., Li, T., Li, D. J. (2024). Fabrication of submicron grained alumina transparent ceramics with high bending strength and low dielectric loss, *Ceramics International,* 50(16), 28301-28308. https://doi.org/10.1016/j.ceramint.2024.05.131

[4] Jing, Y., Tian, F., Guo L., Li, T., Junlin Wu, J., Ivanov, M., Hreniak, D., Li, J. (2024). Effect of TEOS content on microstructure evolution and optical properties of Sm:YAG transparent ceramics, *Optical Materials*, *147*,

114681. https://doi.org/10.1016/j.optmat.2023.114681

[5] Hu, D., Zhang, L., Tian, F., Zhu, D., Chen, P., Yuan, Q., Balabanov, S., Li, J. (2023). Fine-grained transparent Dy_2O_3 ceramics fabricated from precipitated powders without sintering aids, *Optical Materials*, *142*, 114071. https://doi.org/10.1016/j.optmat.2023.114071

[6] Akinribide, O.J., Mekgwe, G. N., Akinwamide, S. O., Gamaoun F., Abeykoon, C., Johnson, O. T., Olubambi, P. A. (2022). A review on optical properties and application of transparent ceramics, *J. Mater. Res. Technol*., 21, 712–738. https://doi.org/10.1016/j.jmrt.2022.09.027

[7] Wan, Z., Li, W., Bei, M., Liu, Z., Yang, Yu. (2020). Fabrication and spectral properties of Ho-doped calcium fluoride transparent ceramics, *Journal of Luminescence,* 223, 117188. https://doi.org/10.1016/j.jlumin.2020.117188

[8] Ye, Y., Tang, Z., Ji, Z., Xiao, H., Liu, Y., Qin, Y., Liang, L., Qi, J., Lu, T. (2021). Fabrication and luminescent properties of holmium doped $Y_2Zr_2O_7$ transparent ceramics as new type laser material, *Optical Materials*, 121, 111643. https://doi.org/10.1016/j.optmat.2021.111643

[9] Ajmala, M., Alib, T., Adil Khana, M., Ahmada, S., Ahmad Mianb, S., Waheeda, A., Ali, S. (2017). Structural and optical properties of La_2O_3:Ho^{3+} and $La(OH)_3$: Ho^{3+} crystalline particles, *Materials Today: Proceedings*, 4 4900–4905. doi.org/10.1016/j.matpr.2017.04.093

[10] Yang, Q., Zhou, H., Xu, J., Su, L. (2008). Synthesis and luminescence characterization of cerium doped Lu_2O_3-Y_2O_3-La_2O_3 solid solution transparent ceramics, *Optics express*., *16*, 12295. doi:10.1364/oe.16.012290.

[11] Le, T. H., Phan, A.-L., Ty, N.M., Zhou, D., Qiu, J., Dan. H.K. (2021). Influences of copper–potassium ion exchange process on the optical bandgaps and spectroscopic properties of Cr^{3+}/Yb^{3+} co-doped in lanthanum aluminosilicate glasses, *RSC Advances, 11*(15), 8917–8926. https://doi.org/10.1039/d0ra10831f

[12] Muller-Buschbaum, Hk., Graebner, P. H. (1971). [Zur Kristallstruktur von $LaErO_3$ und $LaLuO_3$], *Z. Anorg. Allg. Chem*., 386, 158–162 (in German).

[13] Xiong, K., Robertson, J. (2009). Electronic structure of oxygen vacancies in La_2O_3, Lu_2O_3 and $LaLuO_3$, *Microelectr. En.*, *86*(7–9), 1672–1675. https://doi.org/10.1016/j.mee.2009.03.016

[14] Chudinovych, O. V., Zhdanyuk, N.V. (2020). [Interaction of lanthanum oxides and lutetium at a temperature of 1500–1600 °C], *Ukrainian Chem. J.,* 86 (30), 19–25 (in Ukrainian). https://doi.org/10.33609/0041-6045.86.3.2020.19-25

[15] Zinkevich, M. (2007). Thermodynamics of rare earth sesquioxides, *Prog. Mater. Sci*., *52*(4), 597–647. https://doi.org/10.1016/j.pmatsci.2006.09.002.

[16] Coutures, J.P., Foex, M. (1976). Etude a Haute TempCrature des Systsmes Formes par le Sesquioxyde de Lanthane et les Sesquioxydes de Lanthanides. I. Diagrammes de Phases (1400 ◦ C <T<TLiquide), *J. Solid State Chem*., 182(17), 171–182, https://doi.org/10.1016/0022-4596(76)90218-8.

[17] Coutures, J., Sibieude, F., Foex, M. (1976). Etude a haute temp´erature des syst`emes form´espar les sesquioxydes de lanthane avec les sesquioxydes de lanthanides. II. Influence de la trempe sur la nature des phases obtenues `a la temp´erature ambiante, *J. Solid State Chem.*, 17, 377–384, https://doi.org/10.1016/S0022-4596(76)80006-0.

[18] Berndt, V., Maier, D., Keller, C. (1975). New ABO_3 interlanthanide perovskite compounds, *J. Solid State Chem*., 13(1–2), 131–135. https://doi.org/10.1016/0022-4596(75)90090-0.

[19] Korniienko, O.A., Yushkevich, S.V., Bykov, O. I., Sameliuk, A.V., Bataiev, Yu. M., Zamula, M.V. (2023). Phase relation studies in the CeO_2-La_2O_3-Ho_2O_3 system at temperature of 1500 °C, *Mater. Today Commun*., 35, 105789. https://doi.org/10.1016/j.mtcomm.2023.105789

[20] Zhang, Y. (2016*). Thermodynamic Properties of Rare Earth Sesquioxides*, McGill University, Montreal, QC, Canada.

[21] Andrievskaya, E.R. (2010). [*Phase Equilibria in the Systems of Hafnia, Yttria with Rare-Earth Oxides*.] Scientific Book Project, Naukova Dumka, Kiev, 2010. (in Russian).

[22] Zinkevich, M. Thermodynamic Database for Rare Earth Sesquioxide. https://materialsdata.nist.gov/handle/11256/965.

[23] Chudinovych, O. V., Andrievskaya, O. R., Bogatyryova, J. D., Kovylyaev, V. V., Bykov, O. I. (2021). Phase equilibria in the La_2O_3–Y_2O_3–Nd_2O_3 system at 1500 °C, *J. Eur. Ceram. Soc*., 41, 6606–6616. https://doi.org/10.1016/j.jeurceramsoc.2021.06.017

[24] Chudinovych, O. V., Bykov, O. I., Sameliuk, A.V. (2022). Phase equilibria in the La_2O_3–Y_2O_3–Gd_2O_3 system at 1500 °C, *Process. Appl. Ceram.*, *16*(4), 328–334. doi.org/10.2298/PAC2204328C

[25] Chudinovych, O. V., Bykov, O. I., Sameliuk, A.V. (2021). Interaction of lanthanum, lutetium, and ytterbium oxides at 1600 °C, *Powder Metallurgy and Metal Ceramics*., *60*(5-6), 337–346. https://doi.org/10.1007/s11106-021-00248-8

[26] Chudinovych, O. V., Bykov, O. I., Sameliuk, A.V. (2021). Phase relation studies in the La_2O_3–Lu_2O_3–Yb_2O_3 system at 1500 °C, *Journal of Chemistry and Technologies*, *29*(4), 485–494. doi.org/10.15421/jchemtech.v29i4.238943

[27] Chudinovych, O. V., Shyrokov, O. V., Sameliuk, A.V. (2023). Phase equilibria in the La_2O_3–Lu_2O_3–Er_2O_3 system at 1500 and 1600 °C, *Journal of chemistry and technologies*, *31*(1), 51–60. doi:10.15421/jchemtech.v31i1.27149